Inorg. Chem. **2004**, *43*, 5973–5980

Complex Reduction Chemistry of (abpy)$PtCl_2$, abpy = 2,2′-Azobispyridine: Formation of Cyclic $[(\mu,\eta^2{:}\eta^1\text{-abpy})PtCl]_2^{2+}$ with a New Coordination Mode for abpy and a Near-Infrared Ligand-to-Ligand Intervalence Charge Transfer Absorption of the One-Electron Reduced State

Akbey Dogan,[†] Biprajit Sarkar,[†] Axel Klein,[†] Falk Lissner,[†] Thomas Schleid,[†] Jan Fiedler,[‡] Stanislav Záliš,[‡] Vimal K. Jain,[§] and Wolfgang Kaim*[,†]

Institut für Anorganische Chemie, Universität Stuttgart, Pfaffenwaldring 55, D-70550 Stuttgart, Germany, J. Heyrovský Institute of Physical Chemistry, Academy of Sciences of the Czech Republic, Dolejškova 3, CZ-18223 Prague, Czech Republic, and Novel Materials & Structural Chemistry Division, Bhabha Atomic Research Centre, Mumbai - 400085, India

Received January 14, 2004

The structurally characterized (abpy)$PtCl_2$, abpy = 2,2′-azobispyridine, reveals a strong metal/ligand π interaction as supported by DFT calculations. Unexpectedly, its chemical or electrochemical reduction occurs irreversibly to yield EPR-detectable $\{(\mu,\eta^2{:}\eta^2\text{-abpy})[PtCl_2]_2\}^{\bullet-}$ and, as the main product of chloride dissociation, the structurally identified and DFT-calculated dinuclear $[(\mu,\eta^2{:}\eta^1\text{-abpy})PtCl]_2^{2+}$ with a novel coordination mode for abpy and isolated as tetrachlorozincate. Stepwise reversible one-electron reduction of that dimer, separated by 0.24 V, exhibits an intense near-infrared band for the monocationic intermediate $[(abpy^{-I})(abpy)Pt_2Cl_2]^{\bullet+}$ at 1220 nm (ϵ = 3370 M^{-1} cm^{-1}) which is attributed to a ligand-to-ligand intervalence charge-transfer transition.

Introduction

Complexes between dichloroplatinum(II) and chelating aromatic N-heterocycles have been investigated for a number of reasons:

(i) The planarity of such molecules makes them good candidates for π stacking which can occur in various ways.[1−3]

(ii) Luminescence in the solid state or in solution has been observed to occur from metal-to-ligand charge transfer (MLCT) or intraligand $\pi\rightarrow\pi^*$ excited states.[4]

(iii) Although reversible reduction is usually ligand-based (formation of anion radical intermediates) it often leads to well observable ^{195}Pt hyperfine coupling in the EPR spectra due to sizable metal/ligand interaction.[3,5,6]

(iv) Chloroplatinum(II) complexes of nitrogen ligands continue to be major drug targets for tumor therapy.[7]

(v) Some derivatives, most notably (bpym)$PtCl_2$ (bpym = 2,2′-bipyrimidine), have become renowned as precursors for rather efficient catalysts of methane oxidation.[8,9]

* To whom correspondence should be addressed. E-mail: kaim@iac.uni-stuttgart.de.
[†] Universität Stuttgart.
[‡] J. Heyrovský Institute.
[§] Bhabha Atomic Research Centre.

(1) (a) Connick, W. B.; Marsh, R. E.; Schaefer, W. P.; Gray, H. B. *Inorg. Chem.* **1997**, *36*, 913. (b) Connick, W. B.; Henling, L. M.; Marsh, R. E.; Gray, H. B. *Inorg. Chem.* **1996**, *35*, 6261.
(2) Textor, V. M.; Oswald, H. R. *Z. Anorg. Allg. Chem.* **1974**, *407*, 244.
(3) Kaim, W.; Dogan, A.; Wanner, M.; Klein, A.; Tiritiris, I.; Schleid, T.; Stufkens, D. J.; Snoeck, T. L.; McInnes, E. J. L.; Fiedler, J.; Zalis, S. *Inorg. Chem.* **2002**, *41*, 4139.
(4) Connick, W. B.; Miskowski, V. M.; Houlding, V. H.; Gray, H. B. *Inorg. Chem.* **2000**, *39*, 2585.
(5) (a) MacGregor, S. A.; McInnes, E. J. L.; Sorbie, R. J.; Yellowlees, L. J. In *Molecular Electrochemistry of Inorganic Bioinorganic and Organometallic Compounds*; Pombeiro, A. J. L., McCleverty, A. J., Eds.; Kluwer Academic Publishers: Dordrecht, The Netherlands, 1993; p 503. (b) Collison, D.; McInnes, E. J. L.; Mabbs, F. E.; Taylor, K. J.; Welch, A. J.; Yellowlees, L. J. *J. Chem. Soc., Dalton Trans.* **1996**, 329. (c) McInnes, E. J. L.; Farley, R. D.; Macgregor, S. A.; Taylor, K. J.; Yellowlees, L. J.; Rowlands, C. C. *J. Chem. Soc., Faraday Trans.* **1998**, *94*, 2985. (d) McInnes, E. J. L.; Farley, R. D.; Rowlands, C. C.; Welch, A.; Rovatti, L.; Yellowlees, L. J. *J. Chem. Soc., Dalton Trans.* **1999**, 4203. (e) Cf. also a study on [(terpy)PtCl]$^{\bullet}$: Hill, M. G.; Bailey, J. A.; Miskowski, V. M.; Gray, H. B. *Inorg. Chem.* **1996**, *35*, 4585.
(6) For organometallic analogues see: (a) Vogler, C.; Schwederski, B.; Klein, A.; Kaim, W. *J. Organomet. Chem.* **1992**, *436*, 367. (b) Braterman, P. S.; Song, J.-I.; Wimmer, F. M.; Wimmer, S.; Kaim, W.; Klein, A.; Peacock, R. D. *Inorg. Chem.* **1992**, *31*, 5084. (c) Kaim, W.; Klein, A. *Organometallics* **1995**, *14*, 1176.
(7) *Cisplatin*; Lippert, B., Ed.; Wiley-VCH: Weinheim, Germany, 1999.

10.1021/ic049941t CCC: $27.50
Published on Web 08/24/2004

Although Cl_2Pt and the related organoplatinum moieties R_2Pt have been studied with a number of different "polypyridine" π acceptor ligands[6c,10,11] there have not been many reports on such complexes with ligands containing the N═N group.[6a] Platinum(II) compounds containing azo functions have been investigated e.g. by the groups of Kisch and Nishihara in the context of photoinduced isomerization;[12,13] however, Pt^{II} complexes of the recently reviewed 2,2′-azobispyridine (abpy) ligand[14] have not yet been reported. In this work we describe the unusually complex reaction sequence following the reduction of the new mononuclear compound (abpy)$PtCl_2$.

Experimental Section

Instrumentation. EPR spectra were recorded in the X band on a Bruker System ESP 300 equipped with a Bruker ER035M gaussmeter and a HP 5350B microwave counter. ^{1}H NMR spectra were taken on a Bruker AC 250 spectrometer. UV/vis/NIR absorption spectra were recorded on a Bruins Instruments Omega 10 spectrophotometer. ^{195}Pt{^{1}H}-NMR spectra were recorded on a Bruker DPX-300 spectrometer operating at 64.52 MHz employing Na_2PtCl_6 in D_2O as an external standard. Cyclic voltammetry was carried out at 100 mV/s scan rate in 0.1 M Bu_4NPF_6 and approximately 10^{-3} M sample solutions at room temperature (24° ± 2 °C) or other specified temperatures using a three-electrode configuration (glassy carbon electrode with 3 mm diameter, Pt counter electrode, Ag/AgCl reference) and a PAR 273 potentiostat and function generator. The ferrocene/ferrocenium couple served as internal reference. Spectroelectrochemical measurements (in CH_2Cl_2 or DMF/0.1 M Bu_4NPF_6) were performed using an optically transparent thin-layer electrode (OTTLE) cell[15] for UV/vis/NIR spectra and a two-electrode capillary for EPR studies.[16]

Syntheses. (abpy)$PtCl_2$. A mixture containing 200 mg (0.47 mmol) of $(DMSO)_2PtCl_2$[17] and 240 mg (1.30 mmol) of abpy[14] in 50 mL of nitromethane was heated to reflux for 5 h. After removal of solvent from the brown solution recrystallization from nitromethane/diethyl ether and drying under vacuum yielded 187 mg (88%) of dark-red crystals. Anal. Calc. for $C_{10}H_8Cl_2N_4Pt$ (450.19): C, 26.68; H, 1.79; N, 12.45. Found: C, 26.58; H, 1.68; N, 12.18%. ^{1}H NMR (DMSO-d_6): δ = 9.54 (d, 5.6 Hz, ^{3}J(Pt−H) = 34 Hz; H-6); 8.99 (d, 8.0 Hz, H-6′); 8.65 (d, 7.5 Hz, H-3′); 8.63 (t, 5.5 Hz, H-4); 8.33 (t, 6.5 Hz, H-5); 8.16 (t, 7.8 Hz, H-5′); 7.81 (d, 8.0 Hz, H-3); 7.66 (t, 6.4 Hz, H-4′) (each integrating to one proton). ^{195}Pt-NMR (DMSO-d_6): −2110 ppm.

Table 1. Crystallographic and Refinement Data

	(abpy)$PtCl_2$	{[(abpy)$PtCl]_2$}($ZnCl_4$)·$2C_3H_6O$
empirical formula	$C_{10}H_8Cl_2N_4Pt$	$C_{26}H_{28}Cl_6N_8O_2Pt_2Zn$
fw	450.19	1152.82
T (K)	173(2)	293(2)
crystal system	orthorhombic	monoclinic
space group	Pbca	$P2_1/c$
a (Å)	9.1999(2)	10.378(2)
b (Å)	16.6334(5)	14.727(3)
c (Å)	16.1756(4)	22.318(3)
β (deg)	90	93.306(14)
V (Å^3)	2475.3(2)	3405.1(10)
Z	8	4
ρ_{calcd} (g cm^{-3})	2.416	2.592
μ (mm^{-1})	11.750	12.407
GOF	1.160	0.680
final R indices [$I > 2\sigma(I)$][a]	$R_1 = 0.043$	$R_1 = 0.036$
R indices (all data)[a]	$R_W = 0.079$	$R_W = 0.090$

[a] $R_1 = (\sum||F_o| - |F_c||)/\sum|F_o|$. $R_w = \{\sum[w(|F_o|^2-|F_c|^2)^2]/\sum[w(F_o^2)^2]\}^{1/2}$.

{**[(abpy)$PtCl]_2$}($ZnCl_4$).** A mixture of 108 mg (0.240 mmol) of (abpy)$PtCl_2$ in 40 mL of acetone was treated with excess zinc dust (1.08 g, 16.5 mmol). The reddish-brown solution was stirred for 30 min under slow addition of 1.2 g of concentrated hydrochloric acid. The solution was then filtered, reduced to about 10 mL, and treated with diethyl ether to produce a brown precipitate. Washing with acetone and water, drying under vacuum, and recrystallization from nitromethane yielded 34 mg (27%) of brown crystals. Anal. Calc. for $C_{20}H_{16}Cl_6N_8Pt_2Zn$ (1036.65): C, 23,17; H, 1.56; N, 10.81. Found: C, 22.98; H, 1.48; N, 10.46%. ^{1}H NMR (acetone-d_6): δ = 8.85 (dd, 1H, H-6), 7.8−7.71 (m, 2H, H-5, H-6′), 7.59 (ddd, 1H, H-4), 7.16−7.08 (m, 2H, H-3, H-3′), 6.77 (ddd, 1H, H-4′), 6.43 ppm (d, 1H, H-5′); J = 5.4 (H-5, H-6), 6.8 (H-4, H-5), 1.7 (H-3, H-5), 8.3 (H-3, H-4), 1.9 (H-4, H-6), 1.5 (H-4′, H-6′), 7.1 (H-5′, H-6′), 41 Hz (^{195}Pt, H-6).

Crystallography. Single crystals were obtained through slow evaporation of solutions in nitromethane ((abpy)$PtCl_2$) or acetone (dinuclear complex). X-ray data of a red crystal of (abpy)$PtCl_2$ were collected on a Kappa CCD diffractometer (Bruker AXS); data for [(μ-abpy)PtCl)]$_2$($ZnCl_4$)·$2C_3H_6O$ were obtained with a Siemens P4 diffractometer using Mo Kα radiation (λ = 0.71073 Å). The unit cell parameters (Table 1) were determined from 25664 reflections ((abpy)$PtCl_2$) or 8178 reflections (dinuclear complex). The intensity data were corrected for Lorentz-polarization and absorption effects.[18] The structures were solved by direct methods using the SHELX-97 program[19] as part of SHELXTL 5.1[20] for (abpy)$PtCl_2$ and for the dinuclear

(8) (a) Periana, R. A.; Taube, D. J.; Gamble, S.; Taube, H.; Satoh, T.; Fujii, H. *Science* **1998**, *280*, 560. (b) Kua, J.; Xu, X.; Periana, R. A.; Goddard, W. A., III *Organometallics* **2002**, *21*, 511.
(9) Seidel, S.; Seppelt, K. *Inorg. Chem.* **2003**, *42*, 3846.
(10) (a) Braterman, P. S.; Song, J.-I.; Vogler, C.; Kaim, W. *Inorg. Chem.* **1992**, *31*, 222. (b) Klein, A.; van Slageren, J.; Zális, S. *Eur. J. Inorg. Chem.* **2003**, 1917.
(11) (a) Scott, J. D.; Puddephatt, R. J. *Organometallics* **1983**, *2*, 1643. (b) Scott, J. D.; Puddephatt, R. J. *Organometallics* **1986**, *5*, 2522.
(12) Kirsch, H.; Holzmeier, P. *Adv. Organomet. Chem.* **1992**, *34*, 67.
(13) Yukata, T.; Mori, I.; Kurihara, M.; Mizutani, J.; Tamai, N.; Kawai, T.; Irie, M.; Nishihara, H. *Inorg. Chem.* **2002**, *41*, 7143.
(14) Kaim, W. *Coord. Chem. Rev.* **2001**, *219*−*221*, 463.
(15) Krejcik, M.; Danek, M.; Hartl, F. *J. Electroanal. Chem.* **1991**, *317*, 179.
(16) Kaim, W.; Ernst, S.; Kasack, V. *J. Am. Chem. Soc.* **1990**, *112*, 173.
(17) Price, J. H.; Williamson, A. N.; Schramm, R. F.; Wayland, B. B. *Inorg. Chem.* **1972**, *11*, 1280.
(18) Herrendorf, W.; Bärnighausen, H. *X-SHAPE* (Stoe, Darmstadt (Germany)), based on the Crystal Opimization Program *HABITUS* for Numerical Absorption Correction, Karlsruhe (Germany) 1993, and Giessen (Germany) 1996.
(19) Sheldrick G. M. *SHELX-97*, Program for Crystal Structure Analysis; Universität Göttingen: Göttingen (Germany), 1997.
(20) *SHELXTL 5.1*, Bruker Analytical X-ray Systems, Madison, Wisconsin, 1998.

complex employing full matrix least-squares methods. All non-hydrogen atoms were refined anisotropically. Hydrogen atoms were added using appropriate riding models.

DFT Calculations. Ground-state electronic structure calculations of the platinum complexes and their reduced forms have been performed through density-functional theory (DFT) methods using ADF2002.3[21,22] and Gaussian98[23] program packages. The lowest excited states of the neutral complexes were calculated by the time-dependent DFT (TD-DFT) method.

Within Gaussian 98 quasi-relativistic effective core pseudopotentials and corresponding optimized sets of basis functions[24] were used for the Pt centers, while Dunning's[25] valence double-ζ functions with polarization were used for the H, C, N, and Cl atoms. The "Becke-3-LYP" (B3LYP) potential has been employed.[26] Within the ADF program Slater-type orbital (STO) basis sets of double-ζ quality for H and triple-ζ quality with polarization functions for C, N, Cl, and Pt were used. The inner shells were represented by a frozen core approximation, viz., 1s for C and N, 1s−2p for Cl, and 1s−4d for Pt were kept frozen. The following density functionals were used within ADF: A local density approximation (LDA) with VWN parametrization of electron gas data and functional including Becke's gradient correction[27] to the local exchange expression in conjunction with Perdew's gradient correction[28] to the LDA expression (BP). The scalar relativistic (SR) zero-order regular approximation (ZORA) was used within this study. The **g** tensor was obtained from a spin-nonpolarized wave function after incorporating spin-orbit (SO) coupling. **A** tensors were obtained from spin-unrestricted wave functions using quadruple-ζ basis including core electrons. **A** and **g** tensors were obtained by first-order perturbation theory from the ZORA Hamiltonian in the presence of a time-independent magnetic field and by the UKS−Pauli approach using gauge-including atomic orbitals.[29,30]

Scheme 1

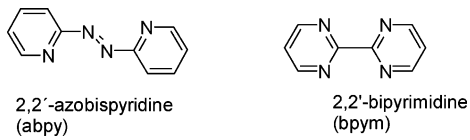

Scheme 2

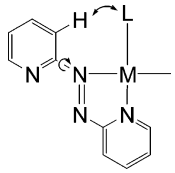

Calculations on (abpy)PtCl$_2$ and [(abpy)PtCl]$_2^{2+}$ were done without any symmetry constraints. Calculations on {(μ-abpy)[PtCl$_2$]$_2$}^{n} were performed in C_s constrained symmetry where the abpy ligand defines the xy plane.

Results and Discussion

Syntheses and Structures. The new mononuclear (abpy)PtCl$_2$ could be obtained from abpy and (DMSO)$_2$PtCl$_2$, (COD)PtCl$_2$, or K$_2$PtCl$_4$ through heating in nitromethane. Despite repeated attempts to obtain dinuclear (μ-abpy)[PtCl$_2$]$_2$ either by prolonged heating of corresponding mixtures in 1:2 molar ratio in noncoordinating solvents such as nitromethane, propylene carbonate, or 1,2-dichlorobenzene or by the reaction of abpy with K[PtCl$_3$(CH$_2$═CH$_2$)] there was no evidence for the formation of the neutral dinuclear (μ-abpy)[PtCl$_2$]$_2$. This result stands in contrast to the eventual success to obtain (μ-bpym)[PtCl$_2$]$_2$;[3] however, it has been noted before[14,31] that the formation of dinuclear complexes of abpy becomes particularly difficult if there is possible interference to overcome between the CH groups in 3,3′ positions and ligands lying in the abpy plane (Scheme 2).

The special π acceptor properties of abpy[14] are evident from ^{195}Pt-NMR spectroscopy. The complex displayed a single resonance at −2110 ppm which compares well with the *cis*-PtCl$_2$N$_2$ motif e.g. in *cis*-[PtCl$_2$(NH$_3$)$_2$] (δ ^{195}Pt = −2097 ppm).[32]

The molecular structure of mononuclear (abpy)PtCl$_2$ as obtained from an X-ray crystal structure analysis (Tables 1 and 2 and Figure 1) exhibits an essentially planar pyridyl/azo/PtCl$_2$ section which adopts a dihedral angle of 61.4° with respect to the second, uncoordinated pyridine ring. The torsion angle N3−N1−C6−N4 is 62.5°. The free 2-pyridyl substituent is twisted to bring the sterically less demanding N atom closer to the metal coordination side without an actual additional coordination; such a behavior has been observed before for mononuclear carbonylmetal compounds of abpy.[31,33]

The structural features of (abpy)PtCl$_2$ including the strong Pt−N$_{azo}$ bond are well reproduced by a DFT calculation (Table 2), the calculated torsion angle N3−N1−C6−N4 is 46.5°.

(21) Fonseca Guerra, C.; Snijders, J. G.; Te Velde, G.; Baerends, E. J. *Theor. Chim. Acc.* **1998**, *99*, 391.
(22) van Gisbergen, S. J. A.; Snijders, J. G.; Baerends, E. J. *Comput. Phys. Commun.* **1999**, *118*, 119.
(23) Frisch, M. J.; Trucks, G. W.; Schlegel, H. B.; Scuseria, G. E.; Robb, M. A.; Cheeseman, J. R.; Zakrzewski, V. G.; Montgomery, J. A.; Stratmann, R. E.; Burant, J. C.; Dapprich, S.; Millam, J. M.; Daniels, A. D.; Kudin, K. N.; Strain, M. C.; Farkas, O.; Tomasi, J.; Barone, V.; Cossi, M.; Cammi, R.; Mennucci, B.; Pomelli, C.; Adamo, C.; Clifford, S.; Ochterski, J.; Petersson, G. A.; Ayala, P. Y.; Cui, Q.; Morokuma, K.; Malick, D. K.; Rabuck, A. D.; Raghavachari, K.; Foresman, J. B.; Cioslowski, J.; Ortiz, J. V.; Stefanov, B. B.; Liu, G.; Liashenko, A.; Piskorz, P.; Komaromi, I.; Gomperts, R.; Martin, R. L.; Fox, D. J.; Keith, T.; Al-Laham, M. A.; Peng, C. Y.; Nanayakkara, A.; Gonzalez, C.; Challacombe, M.; Gill, P. M. W.; Johnson, B. G.; Chen, W.; Wong, M. W.; Andres, J. L.; Head-Gordon, M.; Replogle, E. S.; Pople, J. A. *Gaussian 98, Revision A.7*; Gaussian Inc.: Pittsburgh, PA, 1998.
(24) Andrae, D.; Haeussermann, U.; Dolg, M.; Stoll, H.; Preuss, H. *Theor. Chim. Acta* **1990**, *77*, 123.
(25) Woon, D. E.; Dunning, T. H., Jr. *J. Chem. Phys.* **1993**, *98*, 1358.
(26) Stephens, P. J.; Devlin, F. J.; Cabalowski, C. F.; Frisch, M. J. *J. Phys. Chem.* **1994**, *98*, 11623.
(27) Becke, A. D. *Phys. Rev. A* **1988**, *38*, 3098.
(28) Perdew, J. P. *Phys. Rev. A* **1986**, *33*, 8822.
(29) van Lenthe, E.; van der Avoird, A.; Wormer, P. E. S. *J. Chem. Phys.* **1998**, *108*, 4783.
(30) van Lenthe, E.; van der Avoird, A.; Wormer, P. E. S. *J. Chem. Phys.* **1997**, *107*, 2488.
(31) Kaim, W.; Kohlmann, S.; Jordanov, J.; Fenske, D. *Z. Anorg. Allg. Chem.* **1991**, *598/599*, 217.
(32) Kerrison, S. J. S.; Sadler, P. J. *J. Chem. Soc., Chem. Commun.* **1977**, 861.
(33) Hartmann, H.; Scheiring, T.; Fiedler, J.; Kaim, W. *J. Organomet. Chem.* **2000**, *604*, 267.

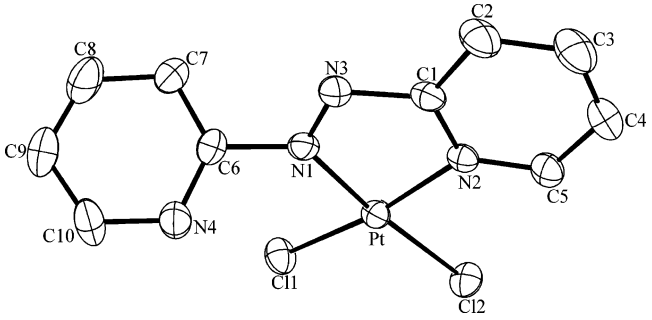

Figure 1. Molecular structure of (abpy)$PtCl_2$ in the crystal crystal (H atoms omitted for clarity).

Table 2. Experimental[a] and DFT-Calculated[b] Bond Parameters of $[(abpy)PtCl_2]^{o/-}$

	neutral		anion
	calc.	exp.	calc.
Pt−N1	1.983	1.955(6)	2.040
Pt−N2	2.017	2.016(6)	2.016
Pt−Cl1	2.286	2.288(2)	2.340
Pt−Cl2	2.288	2.291(2)	2.352
N1−N3	1.292	1.281(8)	1.345
N1−C6	1.441	1.454(9)	1.411
N2−C1	1.373	1.342(9)	1.390
N2−C5	1.348	1.331(9)	1.352
N3−C1	1.371	1.399(10)	1.344
C1−C2	1.398	1.378(11)	1.417
C2−C3	1.400	1.389(13)	1.376
C3−C4	1.388	1.352(12)	1.413
C4−C5	1.389	1.376(10)	1.388
C6−N4	1.331	1.308(10)	1.352
C10−N4	1.338	1.338(11)	1.341
C6−C7	1.395	1.369(11)	1.414
C7−C8	1.392	1.385(11)	1.387
N1−Pt−N2	77.7	78.1(2)	78.2
N1−Pt−Cl1	97.9	96.3(2)	99.8
N1−Pt−Cl2	172.4	173.2(2)	171.6
N2−Pt−Cl2	94.8	95.1(2)	93.5
Cl−Pt−Cl2	89.6	90.6(1)	88.5
Pt−N1−C6	127.3	127.1(5)	129.6
Pt−N1−N3	119.5	120.1(5)	116.4
Pt−N2−C1	111.9	111.6(5)	112.0
Pt−N2−C5	128.7	128.9(5)	128.5

[a] Bond lengths in Å, bond angles in deg. [b] From ADF/BP calculations.

Table 2 also shows the calculated structure parameters for monoanionic $[(abpy)PtCl_2]^{\bullet-}$. The largest changes on electron acquisition include the lengthening (and weakening) of the N1−N3, Pt−N1, and Pt−Cl bonds by about 0.05, 0.06, and 0.06 Å, respectively. While the lengthening of the N−N bond is expected for a reduced azo compound,[34] the significance of the Pt−Cl bond weakening became apparent during further studies. The calculated frontier MOs of (abpy)$PtCl_2$ (Table 3) confirm two π*(abpy) orbitals as LUMO and SLUMO of the complex, while the highest occupied MOs have PtCl character.

Unexpectedly, the one-electron reduced species $[(abpy)PtCl_2]^{\bullet-}$ was not observed experimentally due to rapid irreversible follow-up reactions as confirmed electrochemically (cf. below); attempts to chemically reduce (abpy)$PtCl_2$ using Zn/HCl resulted in the dissociation of chloride (cf. the Pt−Cl bond lengthening on electron acquisition) and in the formation of a new dinuclear compound, identified as $[(\mu,\eta^2{:}\eta^1\text{-abpy})PtCl]_2(ZnCl_4)$ through structure analysis, NMR spectroscopy and confirmed by DFT calculations (Tables 1 and 4, Figure 2). The assumed reaction pathway will be discussed later following electrochemical and spectroscopic studies (cf. below, Scheme 3).

Table 3. ADF/BP Calculated One-Electron Energies and Percentage Composition of Selected Frontier MOs of (abpy)$PtCl_2$ Expressed in Terms of Composing Fragments

MO	E (eV)	predominant character	Pt	abpy	Cl (total)
		Unoccupied			
61a	−2.28	abpy (π_3*)		98 (π*)	
60a	−2.47	abpy + Pt + Cl	29	42	26
59a	−2.96	abpy (π_2*)		98 (π*)	1
58a	−4.50	abpy (π_1*)	14	80 (π*)	6
		Occupied			
57a	−5.63	Cl + Pt	38	4	58
56a	−5.76	Cl + Pt	28	1	70
55a	−6.16	Cl	5	1	93
54a	−6.25	Cl + Pt + abpy	20	53	26
53a	−6.46	Pt	98		
52a	−6.80	abpy	1	98	

The hitherto not observed[14] $\mu,\eta^2{:}\eta^1$-coordination mode of abpy allows it to bridge two Pt^{II} centers in an unsymmetrical fashion. The approximately planar chloro(2-pyridylazo)-platinum(II) motif from the (abpy)$PtCl_2$ precursor has been retained; however, the second chloride ligand (trans to 2-pyridyl) is now replaced by the formerly free 2-pyridyl group of another molecule, yielding a metallacyclic structure involving a puckered eight-membered ring. The bond angles within that ring are ca. 98° at Pt, about 115° at C, and ca. 123° at the N atoms. The dihedral angle between the two chloro(2-pyridylazo)Pt^{II} planes is 68.7°, that between the 2-pyridyl substituents 45.1°. The dihedral angles between the chloro(2-pyridylazo)Pt^{II} planes and the corresponding covalently connected 2-pyridyl substituents within the same ligand are 63.9° and 65.2° which compare with 61.4° for (abpy)$PtCl_2$. A virtually perpendicular arrangement is found at 88.2° and 85.6° between the chloro(2-pyridylazo)Pt^{II} planes and the coordinated 2-pyridyl groups from the other ligand. There are relatively short but clearly nonbonding distances of 3.482 Å between the two Pt centers and of 3.82 Å between the two coordinated azo nitrogen atoms, signifying the possibility for electronic interaction (cf. below) but excluding the accommodation of guest molecules. Larger platinum-containing metallocycles (molecular squares and rectangles) involving heterocyclic acceptor bridges have been poineered by Stang and co-workers.[35]

Similarly as for (abpy)$PtCl_2$ the shorter Pt−N bonds (1.96 Å) are to the azo group, while the Pt−N bonds to the mutually trans-positioned 2-pyridyl rings differ, with about 2.00 Å for the bond to the azo-conjugated pyridyl group and rather long distances at about 2.05 Å for the bond to the twisted pyridine-N. The retained chloride ligands are in trans positions to the coordinated azo nitrogen atoms to allow for the formation of the eight-membered ring structure.

(34) Doslik, N.; Sixt, T.; Kaim, W. *Angew. Chem.* **1998**, *110*, 2521; *Angew. Chem., Int. Ed. Engl.* **1998**, *37*, 2403.

(35) (a) Kryschenko, Y. K.; Seidel, S. R.; Muddiman, D. C.; Nepomuceno, A. I.; Stang, P. J. *J. Am. Chem. Soc.* **2003**, *125*, 9647. (b) Seidel, S. R.; Stang, P. J. *Acc. Chem. Res.* **2002**, *35*, 972.

Scheme 3

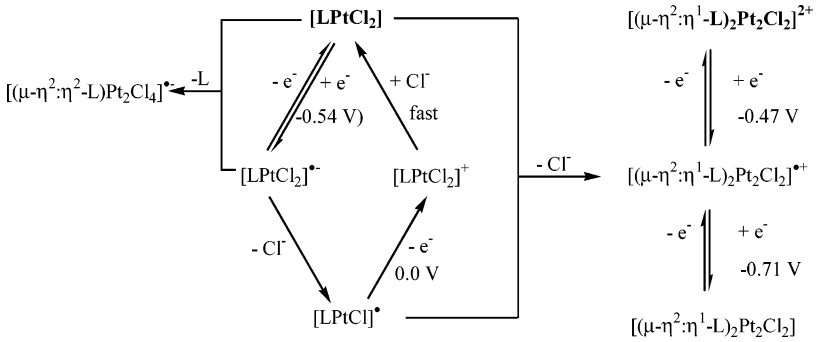

Table 4. Selected Experimental[a] and DFT-Calculated[b] Bond Parameters of $\{[(\mu,\eta^2{:}\eta^1\text{-abpy})PtCl]_2\}^{2+/+}$

	(2+)		(+)
	calc.	exp.	calc.
Pt1−N1, Pt2−N5	1.987	1.959(6), 1.952(6)	2.000
Pt1−N2, Pt2−N6	2.022	2.004(6), 1.995(6)	2.012
Pt1−N8, Pt2−N4	2.065	2.035(6), 2.051(6)	2.064
Pt1−Cl1, Pt2−Cl2	2.277	2.276(2), 2.281(2)	2.302
N1−N3, N5−N7	1.289	1.261(9), 1.262(8)	1.312
N1−Pt1−N2, N5−Pt2−N6	77.3	77.1(2), 77.7(2)	77.6
N1−Pt1−N8, N5−Pt2−N4	99.1	98.5(2), 97.8(2)	99.5
N2−Pt1−Cl1, N6−Pt2−Cl2	96.1	97.13(18), 96.91(19)	95.5
N8−Pt1−Cl1, N4−Pt2−Cl2	87.3	87.05(18), 87.67(17)	87.4
N1−Pt1−N8−C16, N5−Pt2−N4−C6	92.0	91.7(6), 93.5(6)	102.5
Pt1−N1−C6−N4, Pt2−N5−C16−N8	61.9	62.8(8), 64.2(8)	50.9

[a] Bond lengths in Å, bond angles in deg. [b] From ADF/BP calculations.

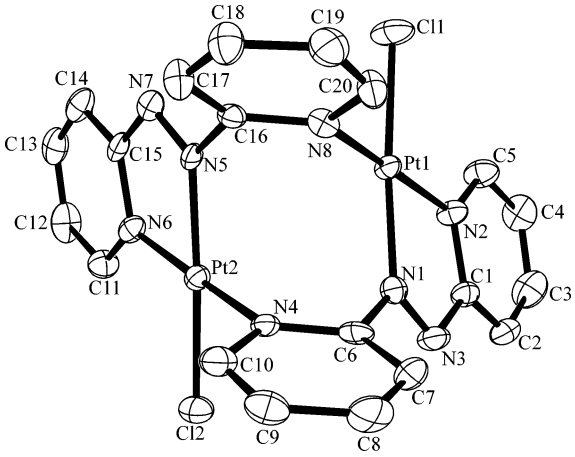

Figure 2. Molecular structure of the dication of $[(\mu,\eta^2{:}\eta^1\text{-abpy})PtCl]_2(ZnCl_4)$ in the crystal (H atoms omitted for clarity).

Cyclic Voltammetry. Mononuclear $(abpy)PtCl_2$ is reduced reversibly at $E_o = -0.54$ V vs $Fc^{+/o}$ in CH_2Cl_2/0.1 M Bu_4NPF_6 at −50 °C; at room temperature this process is reversible only at high scan rates >5 V/s under otherwise identical conditions, becoming irreversible at slower scan rates due to chloride dissociation following the charge transfer (initial EC mechanism). An additional anodic peak at about 0.0 V is observed (Figure S1, Supporting Information). Free chloride anions were identified by their anodic polarographic signature after bulk electrolysis.

This surprising instability of $[(abpy)PtCl_2]^{\bullet-}$ despite the less negative potential[3] is attributed to the considerable labilization of the Pt−Cl bonds as calculated by DFT (cf. above and Table 2), the large effect being associated with the high degree of charge localization at the coordinating

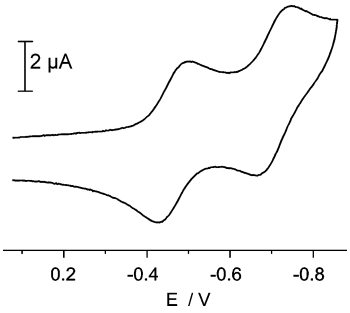

Figure 3. Cyclic voltammogram of $[(\mu,\eta^2{:}\eta^1\text{-abpy})PtCl]_2(ZnCl_4)$ at 0.96 mM concentration in CH_2Cl_2/0.1 M Bu_4NPF_6 at 100 mV/s scan rate (potential vs $[Fe(C_5H_5)_2]^{+/o}$).

nitrogen atoms of $abpy^{\bullet-}$.[14,36] On the other hand, the dimer $[(\mu,\eta^2{:}\eta^1\text{-abpy})PtCl]_2(ZnCl_4)$ isolated after chloride dissociation undergoes two reversible one-electron reduction steps at $E_1 = -0.47$ and $E_2 = -0.71$ V, i.e., separated by 0.24 V in CH_2Cl_2 (Figure 3). This potential difference translates to a comproportionation constant of $K_c = 10^{4.07}$ at 25 °C according to (2), a significant value considering that the abpy ligands and especially the azo groups therein are the main electron accepting sites.

$$\underset{\text{Ox}}{[M_2L_2]^n} \underset{+e^- \ (E_1)}{\overset{-e^-}{\rightleftharpoons}} \underset{\text{Int}}{[M_2L_2]^{n-1}} \underset{+e^- \ (E_2)}{\overset{-e^-}{\rightleftharpoons}} \underset{\text{Red}}{[M_2L_2]^{n-2}} \qquad (1)$$

$$\text{comproportionation constant } K_c = \frac{[\text{Int}]^2}{[\text{Red}][\text{Ox}]} = e^{nF\Delta E/RT} \qquad (2)$$

Spectroelectrochemistry (EPR, UV/vis/NIR). Attempts to detect the radical anion intermediate $[(abpy)PtCl_2]^{\bullet-}$ by

(36) Kaim, W.; Kohlmann, S. *Inorg. Chem.* **1987**, *26*, 68.

Table 5. Experimental[a] and DFT-Calculated[b] Data of Dinuclear Radical Complexes

radical complex	g_1	g_2	g_3	g_{av}	g_1-g_3	$a(^{195}Pt)^a$	ref
$\{(bpym)[PtCl_2]_2\}^{\bullet-}$	2.049	2.008	1.902	1.986	0.147	3.7	3
$\{(abpy)[PtCl_2]_2\}^{\bullet-}$	2.158	2.021	1.910	2.030	0.248	5.8	this work
$\{(abpy)[PtCl_2]_2\}^{\bullet-}$ [b]	2.350	1.964	1.830	2.048	0.520	4.9[c]	this work
$\{(abpy)[PtCl_2]_2\}^{\bullet-}$ [d]	2.321	2.041	1.871	2.078	0.450		this work
$\{[(abpy)PtCl]_2\}^{\bullet+}$ [b]	2.027	2.007	1.960	1.998	0.087	2.7[c]	this work
$\{[(abpy)PtCl]_2\}^{\bullet+}$ [d]	2.019	1.984	1.968	1.990	0.051		this work
$\{(abpy)[IrCl(C_5Me_5)]_2\}^{\bullet+}$	1.979	1.971	1.954	1.968	0.025		39
$\{(abpy)[ReCl(CO)_3]_2\}^{\bullet-}$	2.023	2.007	1.981	2.004	0.042	*e*	40

[a] Coupling constant in mT. [b] Spin-restricted calculations including spin−orbit coupling for *g* values, core electrons included. [c] Spin-unrestricted ZORA calculations, core electrons included. [d] Spin-unrestricted Pauli calculations for *g* values, frozen core approximation. [e] $a(^{185,187}Re) = 2.54$ mT.

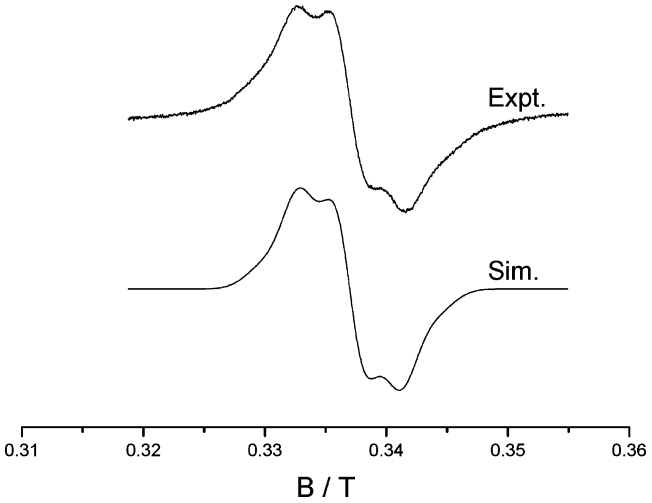

Figure 4. EPR spectrum of $\{(\mu,\eta^2{:}\eta^2\text{-abpy})[PtCl_2]_2\}^{\bullet-}$ with simulation (3.1 mT line width).

EPR through in situ electrolysis of $(abpy)PtCl_2$ produced a room temperature spectrum which could only be simulated assuming the interaction of *two* equivalent platinum atoms (^{195}Pt: I = 1/2, 33.8% natural abundance) with the unpaired electron on the ligand (Figure 4).

We thus conclude that the radical anion $\{(\mu,\eta^2{:}\eta^2\text{-abpy})[PtCl_2]_2\}^{\bullet-}$ of the symmetrical dinuclear complex has been formed in a not unfamiliar electron transfer-induced "polynucleation" side reaction.[37] Apparently the Pt−N bond labilization brought on by reduction (cf. Table 2) facilitates dissociation, while the enhanced basicity of $abpy^{\bullet-}$ favors the coordination of two $PtCl_2$ groups despite steric hindrance.

The isotropic ^{195}Pt hyperfine coupling constant of 5.8 mT lies at the upper end of what has been observed hitherto for platinum(II)-containing radical complexes,[3,6,7,10,11,38] for instance, $\{(\mu,\eta^2{:}\eta^2\text{-bpym})[PtCl_2]_2\}^{\bullet-}$ has $a_{iso}(^{195}Pt) = 3.7$ mT.[3] The comparison in Table 5 of *g* tensor components in the glassy frozen state further confirms the large amount of metal contribution to the singly occupied molecular orbital of $\{(\mu,\eta^2{:}\eta^2\text{-abpy})[PtCl_2]_2\}^{\bullet-}$, the very large *g* anisotropy g_1-$g_3 = 0.248$ being without precedent in related species $(\mu\text{-abpy})[ML_n]_2$ (Tables 5 and 6).[39,40] However, there are diplatinum(II) radical complexes with comparable *g* anisotropy.[38] Both DFT approaches using either spin−orbit coupling within the spin-restricted ZORA or UKS−Pauli calculations overestimate the *g* anisotropy (Table 5) but confirm both the unusually large metal participation at the singly occupied MO (SOMO) and the deviation of g_{iso} to *higher* values relative to *g(electron)* = 2.0023. The latter signifies[41] a doubly occupied orbital lying close to the SOMO which is tentatively attributed to the highest-lying occupied d orbital of Pt^{II} ($5d^8$ configuration).

Table 6. UKS-ZORA Calculated Spin Densities ρ_x of Radical Complexes

x	$[(abpy)PtCl_2]^{\bullet-}$	$[(abpy)Pt_2Cl_4]^{\bullet-}$	$\{[(abpy)PtCl]_2\}^{\bullet+}$
Pt	0.149	0.115	0.020
Cl	0.009	0.010	0.018
N1 (N5)[a] (azo)	0.266	0.187	0.117
N2 (N6)	0.097	0.074	0.043
N3 (N7) (azo)	0.180	0.187	0.131
N4(N8)	0.060	0.074	0.018

[a] Numbering according to structure figures.

One-electron reduction of $[(\mu,\eta^2{:}\eta^1\text{-abpy})PtCl]_2(ZnCl_4)$ by in situ electrolysis or chemical methods at room-temperature did not produce EPR spectra attributable to $\{[(\mu,\eta^2{:}\eta^1\text{-abpy})PtCl]_2\}^{\bullet+}$, even at measurement temperatures down to 4 K. Such a species would have one abpy and one $abpy^{\bullet-}$ ligand with the possibility of rapid electron hopping between equivalent ligands, separated (at the coordinating N_{azo} centers) by only 3.82 Å. Such hopping can cause severe EPR line-broadening,[42] especially if the presence of heavy elements with their high spin−orbit coupling constants contributes further to the broadening of EPR features. In larger metallocycles such as tetranuclear molecular rectangles[43] with reducible π acceptor bridges the hopping can be too slow to

(37) (a) Kaim, W.; Olbrich-Deussner, B.; Gross, R.; Ernst, S.; Kohlmann, S.; Bessenbacher, C. in *Importance of Paramagnetic Organometallic Species in Activation, Selectivity and Catalysis*; Chanon, M., Ed.; Kluwer Academic Publishers: Dordrecht, The Netherlands, 1989; p 283. (b) Gross-Lannert, R.; Kaim, W.; Olbrich-Deussner, B. *Inorg. Chem.* **1990**, *29*, 5046. (c) Bruns, W.; Kaim, W.; Ladwig, M.; Olbrich-Deussner, B.; Roth, T.; Schwederski, B. in *Molecular Electrochemistry of Inorganic, Bioinorganic and Organometallic Compounds;* Pombeiro, A. J. L., McCleverty, J., Eds.; Kluwer Academic Publishers: Dordrecht, The Netherlands (Nato ASI Series C 385), 1993; p 255.

(38) (a) Klein, A.; McInnes, E. J. L.; Scheiring, T.; Zális, S. *J. Chem. Soc., Faraday Trans.* **1998**, 2979. (b) Kaim, W.; Schwederski, B. In *Magnetic Properties of Free Radicals*; Fischer, H., Ed.; *Landolt-Börnstein* II/26a, in print.

(39) Frantz, S.; Reinhardt, R.; Greulich, S.; Wanner, M.; Fiedler, J.; Duboc-Toia, C.; Kaim, W. *Dalton Trans.* **2003**, 3379.

(40) Frantz, S.; Hartmann, H.; Doslik, N.; Wanner, M.; Kaim, W.; Kümmerer, H.-J.; Denninger, G.; Barra, A.-L.; Duboc-Toia, C.; Fiedler, J.; Ciofini, I.; Urban, C.; Kaupp, M. *J. Am. Chem. Soc.* **2002**, *124*, 10563.

(41) Kaim, W. *Coord. Chem. Rev.* **1987**, *76*, 187.

(42) Heilmann, M.; Baumann, F.; Kaim, W.; Fiedler, J. *J. Chem. Soc., Faraday Trans.* **1996**, *92*, 4227.

(43) (a) Kaim, W.; Schwederski, B.; Dogan, A.; Fiedler, J.; Kuehl, C. J.; Stang, P. J. *Inorg. Chem.* **2002**, *41*, 4025. (b) Hartmann, H.; Berger, S.; Winter, R.; Fiedler, J.; Kaim, W. *Inorg. Chem.* **2000**, *39*, 4977.

Table 7. Spectroscopic Data of Platinum Complexes[a]

compound	λ_{max} (ϵ)[b]		
(abpy)$PtCl_2$	395 (9300)	516 (3270)	
$\{[(abpy)PtCl]_2\}^{2+}$	354 (15200)	507 (5200)	
$\{[(abpy)PtCl]_2\}^{\bullet+}$	339 (16900)	485 (9000)	600sh 1220 (3370)
$\{[(abpy)PtCl]_2\}$	338 (24000)	492 (14800)	

[a] From spectroelectrochemistry in DMF/0.1 M Bu_4NPF_6. [b] Wavelengths λ in nm, molar extinction coefficients ϵ in M^{-1} cm^{-1}.

have an effect on the EPR spectra because of the large interligand distances (which also diminish the differences between reduction potentials).[43] From another viewpoint, the degenerate π*(abpy) LUMO is populated by only one electron in $\{[(\mu,\eta^2{:}\eta^1\text{-abpy})PtCl]_2\}^{\bullet+}$ and the dimetallacyclic system does not easily allow for much Jahn-Teller-type distortion to effectively lift the degeneracy. The presence of excited states lying close to the radical ground state in such a situation could thus contribute to rapid relaxation and thus EPR silence even at low temperatures. In comparison to $\{(\mu,\eta^2{:}\eta^2\text{-abpy})[PtCl_2]_2\}^{\bullet-}$ the DFT calculations (Table 5) for the radical cation complex show much smaller g anisotropies g_1-g_3 and g_{iso} closer to the free electron value.

The opportunity to have a ligand-based mixed-valent dimer complex available in a fairly rigid metallacyclic setting has prompted UV/vis/NIR-spectroelectrochemical investigations (Table 7) using an optically transparent thin-layer electrolytic (OTTLE) cell.[15] Whereas the dinuclear precursor $\{[(\mu,\eta^2{:}\eta^1\text{-abpy})PtCl]_2\}(ZnCl_4)$ exhibits only a typical metal-to-ligand charge-transfer band at 507 nm in the visible (DMF/0.1 M Bu_4NPF_6) like the mononuclear (abpy)$PtCl_2$ (516 nm), the one-electron reduced intermediate is distinguished by a rather intense band (ϵ = 3370 M^{-1} cm^{-1}) in the near-infrared (NIR) region at 1220 nm (Figure 5).

In addition, the band around 500 nm intensifies which is attributed to the occurrence of a typical $\pi\rightarrow\pi$* transition of abpy$^{\bullet-}$ (408 nm in noncoordinated abpy$^{\bullet-}$).[14,44] In the two-electron reduced neutral compound $[(\mu,\eta^2{:}\eta^1\text{-abpy})PtCl]_2$ the NIR band disappears, whereas the bands around 490 and 340 nm associated with abpy$^{\bullet-}$ show further increase (Figure 5, Table 7), suggesting an $[(abpy^{-I})Pt^{II}Cl]_2$ oxidation state situation. The transition in the NIR region of $\{[(\mu,\eta^2{:}\eta^1\text{-abpy})PtCl]_2\}^{+}$ is thus interpreted as a ligand-based intervalence charge transfer (IVCT) process π*(abpy$^{\bullet-}$)$\rightarrow\pi$*(abpy).

Although the chemistry, spectroscopic, and theoretical approaches to mixed-valency of chemically equivalent sites in symmetrical molecules has been developed largely for inorganic materials,[45] including ligand-bridged dinuclear metal complexes such as the Creutz-Taube ion,[46] these concepts have been successfully applied also to organic molecules such as stepwise oxidizable bis-amine and bis-hydrazine derivatives.[47] In the present case the stepwise

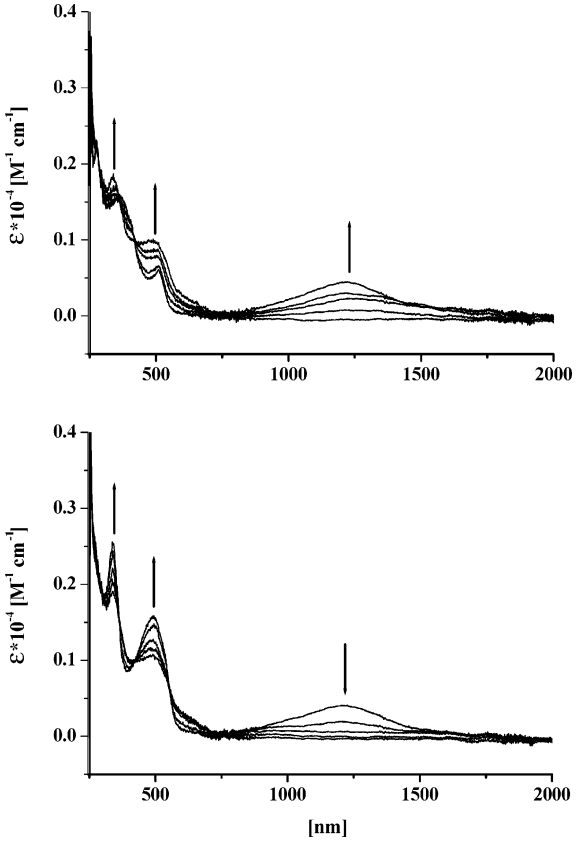

Figure 5. Two-step spectroelectrochemical reduction of $[(\mu,\eta^2{:}\eta^1\text{-abpy})PtCl]_2(ZnCl_4)$ in DMF/0.1 M Bu_4NPF_6 (stepwise potentiostatic regime).

reducible bridging ligands abpy exist in a fairly rigid setting with redox-inactive platinum(II); the observed energy (8200 cm^{-1}), intensity (3370 M^{-1} cm^{-1}), and bandwidth at half-height (2800 cm^{-1}) of the intervalence charge transfer band suggest a relatively large degree of electronic coupling across the distance of about 3.8 Å between the π* MO-dominating azo centers of the abpy ligands. Applying the Hush approximation[48] $\Delta\nu_{1/2}(calc.) = (\nu_{max} \times 2310\ cm^{-1})^{1/2}$ for valence-trapped situations to $\{[(abpy)PtCl]_2\}^{\bullet+}$ gives 4352 cm^{-1}—much higher than the experimentally observed 2800 cm^{-1}. While this result suggests a Class III (valence-averaged) system, the rather low K_c value of $10^{4.07}$ would also be compatible with a Class II (valence-localized) situation.[45,46] Unfortunately, the absence of an EPR signal down to 4 K precluded a direct determination of the valence (de)localization.

The spectral data of (abpy)$PtCl_2$ could be successfully reproduced using TD-DFT methodology (Table 8). The most intense absorption bands are due to allowed metal-to-ligand charge transfer (MLCT) transitions from either metal/chloride mixed or pure metal-centered orbitals to π*(abpy). Spectroelectrochemistry of (abpy)$PtCl_2$ at room temperature also showed the emergence of the 1220 nm band due to the irreversible, i.e., chloride dissociative reduction process mentioned above. The dimer $\{[(abpy)PtCl]_2\}^{\bullet+}$ thus formed at the electrode can be further reduced in the same fashion

(44) Krejcik, M.; Zalis, S.; Klima, J.; Sykora, D.; Matheis, W.; Klein, A.; Kaim, W. *Inorg. Chem.* **1993**, *32*, 3362.
(45) Prassides, K., Ed. *Mixed Valency Systems: Applications in Chemistry, Physics and Biology*; Kluwer Academic Publishers: Dordrecht, The Netherlands, 1991.
(46) Kaim, W.; Klein, A.; Glöckle, M. *Acc. Chem. Res.* **2000**, *33*, 755.
(47) (a) Nelsen, S. F. *Chem. Eur. J.* **2000**, *6*, 581. (b) Lambert, C.; Nöll, G. *J. Am. Chem. Soc.* **1999**, *121*, 8434. (c) Sun, D.-L.; Rosokha, S. V.; Lindeman, S. V.; Kochi, J. K. *J. Am. Chem. Soc.* **2003**, *125*, 15950.
(48) Hush, N. S. *Progr. Inorg. Chem.* **1967**, *8*, 391.

Table 8. Selected Calculated Lowest TD-DFT Singlet Transition Energies and Oscillator Strengths for (abpy)$PtCl_2$

		G98/B3LYP		
state	main character (in %)	trans. energy[a] (wavelength)[a]	osc. str.	experiment λ_{max}/ϵ[b]
^{1}A	(HOMO → LUMO)	2.00 (620)	0.002	
^{1}A	HOMO-3 → LUMO	2.23 (555)	0.004	
^{1}A	(HOMO-2 → LUMO)	2.55 (494)	0.088	516 (3270)
^{1}A	(HOMO-4 → LUMO)	3.09 (405)	0.013	
^{1}A	(HOMO-5 → LUMO)	3.15 (394)	0.134	305 (9300)

[a] Transition energies in eV, wavelengths in nm. [b] Absorption maxima in nm, molar extinction coefficients in M^{-1} cm^{-1}.

as observed with the synthesized complex $[(abpy)PtCl]_2(ZnCl_4)$.

Scheme 3 illustrates the two spectroscopically detected consequences of Pt-donor labilization on reduction, the EPR-detectable formation of dinuclear $\{(\mu\text{-}\eta^2\text{:}\eta^2\text{-abpy})[PtCl_2]_2\}^{\bullet-}$ (via Pt−N dissociation), and the dimerization (3) after chloride loss to $\{[(\mu\text{-}\eta^1\text{:}\eta^2\text{-abpy})PtCl]_2\}^{\bullet+}$ with its intense NIR absorption.

$$2(abpy)PtCl_2 + e^- \rightarrow \{[(abpy)PtCl]_2\}^{\bullet+} + 2Cl^- \quad (3)$$

We have shown that this reaction can also take place with zinc as a chemical reductant (4):

$$4(abpy)PtCl_2 + Zn \rightarrow 2\{[(abpy)PtCl]_2\}^{\bullet+} + [ZnCl_4]^{2-} \quad (4)$$

Oxidation to diamagnetic $\{[(\mu\text{-}\eta^1\text{:}\eta^2\text{-abpy})PtCl]_2\}^{2+}$ and precipitation of the tetrachlorozincate in the presence of excess chloride as HCl produced the isolated and structurally characterized material.

According to Scheme 3, supported by experimental and DFT calculation results, the initial reduction of $(abpy)PtCl_2$ can labilize both the Pt−N and the Pt−Cl bonds. Whereas the former is responsible for the formation of the EPR-detectable dinuclear radical anion complex $\{(\mu,\eta^2\text{:}\eta^2\text{-abpy})[PtCl_2]_2\}^{\bullet-}$, the unexpected[49] Pt−Cl dissociation leads to the NIR-spectroscopically detectable cation radical of the dimer which could be eventually isolated in oxidized form as $[(\mu,\eta^2\text{:}\eta^1\text{-abpy})PtCl]_2(ZnCl_4)$. It is remarkable how reductive

Scheme 4

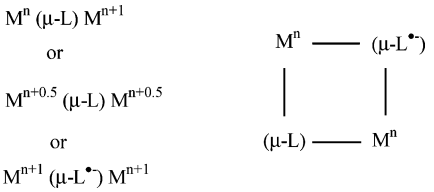

activation causes such a complex sequence for apparently inert platinum(II) complexes; however, the abpy ligand is unusual in several ways:[14] Through its low-lying π^* MO with high contributions from the coordinating nitrogen centers it allows for strong electronic interaction; on the other hand, it offers special steric effects such as its ability to act as a compact bridge, both in the established $\mu,\eta^2\text{:}\eta^2$ mode and, as now shown for the first time, in the $\mu,\eta^2\text{:}\eta^1$ mode.

As Scheme 4 illustrates, mixed-valency in molecule-bridged dinuclear complexes can thus be extended beyond the known alternatives[46] if potentially interacting ligand bridges of metallasupramolecular structures[43] become involved in electron transfer.

Acknowledgment. This work was supported by the Deutsche Forschungsgemeinschaft, the Volkswagenstiftung, and the Fonds der Chemischen Industrie. Further support by the BMBF (project IND 99/060), the European Union (COST action D14), the Grant Agency of the Czech Republic, grant No. 203/03/082, and the Ministry of Education of the Czech Republic, grant COST OC D15.10 is gratefully acknowledged. We also thank Priv.-Doz. Dr. M. Niemeyer for crystallographic data collection and Johnson & Matthey for a loan of platinum compounds.

Supporting Information Available: Figure S1 (cyclic voltammograms of $(abpy)PtCl_2$ at various temperatures) and X-ray crystallographic files in CIF format for $(abpy)PtCl_2$ and $\{[(abpy)PtCl]_2\}(ZnCl_4)\cdot 2C_3H_6O$. This material is available free of charge via the Internet at http://pubs.acs.org.

IC049941T

(49) Reductive labilization of the M-Cl bond is common for M = Pd where it is employed synthetically: Amatore, C.; Jutand, A. *Acc. Chem. Res.* **2000**, *33*, 314. A spectroelectrochemical study of $(abpy)PdCl_2$ is underway.